Available online at www.sciencedirect.com
SCIENCE DIRECT®
International Journal of Pharmaceutics 262 (2003) 109–124
international journal of pharmaceutics
www.elsevier.com/locate/ijpharm

Structural properties of magnesium stearate pseudopolymorphs: effect of temperature

Pierre Bracconi [a,*], Cyrille Andrès [b], Augustin Ndiaye [a,b]

[a] *Laboratoire de Recherches sur la Réactivité des Solides (CNRS UMR 5613), Université de Bourgogne, UFR Sciences et Techniques, 9 avenue Alain Savary, BP 47870, F-21078 Dijon Cedex, France*
[b] *Groupe de Technologie des Poudres à Usage Pharmaceutique, Université de Bourgogne, UFR de Pharmacie, 7 boulevard Jeanne d'Arc, F-21033 Dijon Cedex, France*

Received 21 October 2002; received in revised form 26 March 2003; accepted 18 June 2003

Abstract

A thorough review of the relevant literature reveals that the interaction between water vapour and magnesium stearate, in contrast to many other metal soaps, is not properly understood. The structural modifications associated with the up-take or loss of water of vegetable-derived commercial magnesium stearate powders exposed to humid air or vacuum at room temperature are investigated using standard powder X-ray diffractometry. It is found that in such conditions magnesium stearate reacts reversibly with the vapour phase with structural consequences very similar to the high temperature transition between the crystalline and rotator phases of other anhydrous metal soaps. When temperature is increased under dry nitrogen the diffraction band characteristic of the rotator phase shifts towards higher angle values an the corresponding lattice spacing increases at the rate of $6.9 \times 10^{-4}\,C^{-1}$. Melting takes place gradually above 100 °C as revealed by the collapse of the diffraction band and the growth of the broader diffusion band characteristic of the liquid state. Full clarification of the structure of the hydrated and dried phases proves impossible based on powder diffraction spectra obtained with conventional high resolution X-ray diffraction equipment.

Keywords: Magnesium stearate; Hydrates; Anhydrate; Reactivity; Structure

1. Introduction

Magnesium stearate is in widespread use as gelling, sanding and anti-sticking agents, stabiliser, lubricant, emulsifier and plasticiser for polymers, in the paint, food, rubber, paper and pharmaceutical industries. Its production by some 195 companies throughout the world is essentially based either on the reaction of stearic acid with a magnesium compound such as carbonate, oxide ... or on the reaction of magnesium chloride with sodium or ammonium stearate in aqueous solution leading to the precipitation of the dihydrate $C_{36}H_{70}MgO_4{\cdot}2H_2O$. In the field of drug manufacturing, where it is mainly used as a solid lubricant, its lubricating capacity and overall activity in the various pharmaceutical forms in which it is incorporated may vary from one producer to another (Barra and Somma, 1996; Brittain, 1989) and even sometimes from one batch to another of the same origin. The drying process of the precipitated dihydrate phase is regarded as a potential source of such differences (Müller, 1977a) for the thermal stability of the various structures of concern is quite limited. This last point is revisited and

* Corresponding author. Tel.: +33-380-396154; fax: +33-380-396132.
E-mail address: pierre.bracconi@u-bourgogne.fr (P. Bracconi).

0378-5173/$ – see front matter © 2003 Elsevier B.V. All rights reserved.
doi:10.1016/S0378-5173(03)00339-9

clarified by the results presented in the following sections.

It must be emphasised that commercial magnesium stearate is not certified as a high purity single phase material of the kind used in fundamental investigations. As an example, the European pharmacopoeia (European Pharmacopeia, 2002) specifies that "Magnesium stearate is a mixture of magnesium salts of different fatty acids, mainly stearic and palmitic, and of others in lower proportions. The magnesium weight fraction in the dried substance, is 4% at the least and 5% at the most. The fraction of fatty acid contains at least 40% of stearic acid, and 90% of stearic and palmitic acids altogether". Indeed, this should be regarded as *minimal* requirements.

It is somewhat surprising that the crystalline structure of that particular material and its modification by interaction with water vapour are not well established as they are for some other metal-soaps. The very reason for this is that single crystals of sufficient quality of either the hydrate or anhydrate phases could never been produced so that all published data relating to the structure of magnesium stearate, including the present work, are derived from powder diffraction spectra. And the latter prove particularly inadequate for structure determination due to the overlapping of [0 0 *l*] reflections from the two crystallised structures and the difficulty of preparing single phase samples. In relation, it may be mentioned here that Vand failed to index the powder diffraction pattern he reported for magnesium stearate (ASTM, 1965) whereas he succeeded with many other metal soaps by using the graphical methods known by his name (Vand, 1948a,b).

Indeed, it has been recognised for a long time that magnesium stearate can exist at room temperature as distinct phases differing by their water content and by the length of a so-called long interplanar spacing (Vold and Hattiangdi, 1949). Even though the respective structures have not been fully established in terms of a unit cell and lattice parameter values, their general characteristics as described by Müller (1977b,c) and by Sharpe et al. (1997), for instance, are accepted because they fit in the general description of established structures of other metal-soaps and lipids (Small, 1986). The X-ray powder diffraction spectra corresponding to the di- and trihydrates and to a so-called anhydrous form have been reported by various authors. Though, from one report to another, they may differ from two standpoints:

(1) The precise angular position of the low angle reflections, recognised as harmonics of the [0 0 1] reflection (which is usually not observed).
(2) The *number* and *intensity* of reflections corresponding to smaller "side spacing" (Vold and Hattiangdi, 1949; Müller et al., 1982; Brittain, 1989; Leinonen et al., 1992; Sharpe et al., 1997). One striking example among many of such discrepancies may be found when comparing the spectra of the (allegedly) pure dihydrate phase published by Rajala and Laine (1995) on the one hand, and Sharpe et al. (1997) on the other. They differ by the positions and relatives intensity of most reflections (numerical values can be found in table of appendix) and the $d_{0\,0\,1}$ spacing values inferred from these differ by as much as 8%.

In fact, agreement between the various tentative interpretations of the reported diffraction spectra by their respective authors essentially reduces to the recognition of the low angle reflections as successive harmonics of the long interplanar spacing $d_{0\,0\,1}$. Müller (1977a) tried to infer the unit cell symmetry and lattice parameter values by computerised refining methods. He could only propose two possible and equally probable structures, monoclinic and orthorhombic, for the same hydrate phase. He also observed variations of the structural data with particle shape and water content. Numerical values of the lattice parameters are given for the monoclinic solutions only. For needle-shaped particles with composition close to that of the trihydrate, $a = 7.0$ Å, $b = 7.4$ Å, $c = 53.9$ Å and $\beta = 118.7^\circ$. For lamellas with water content between 1 or 2 H_2O per mole stearate, $a = 5.9$ Å, $b = 7.9$ Å, $c = 53.2$ Å and $\beta = 97.9^\circ$. In contrast, Marwaha and Rubinstein (1988) described a triclinic unit cell with totally different parameter values as representative of the structure of a mixed 15–85% stearate-palmitate of magnesium. However, all these authors failed to present any direct evidences, such as indexed diffraction spectra (in the small side-spacings range).

High temperature *anhydrous* phases of magnesium stearate have been described by Spegt and Skoulios (1962). It is important to mention that these authors investigated a commercial material that they thoroughly washed in boiling alcohol, then in ether, and

finally dried at 110 °C in vacuum. Three structures were identified. Up to 110 °C, a crystalline phase (noted A) is characterised by a layered structure with an interlayer spacing equal to 47.5 Å. No additional description or interpretation is given except that it is *similar* to the more documented structure of the homologous A phase of Ca-stearate (Spegt and Skoulios, 1960). The latter is specifically characterised by *fine* diffraction bands in the interval of short *d*-spacing values 3–5 Å. The structure of phase B of the Ca-soap (Spegt and Skoulios, 1964) is still layered (harmonics 1, 2 and 3 are detected), but the *fine* diffraction band in the diffraction spectrum of phase A is now replaced by a *diffuse* band centred at 4.18 Å, typical of liquid paraffin. Notice here that phase B in Spegt and Skoulios (1960) is labelled phase C in Spegt and Skoulios (1964). These properties of the Ca-stearate phases A and B just mentioned appear of great relevance here because they mimic closely the changes we observe with magnesium stearate when its water content is varied at room temperature (Section 2).

The B phase of the magnesium soap (Spegt and Skoulios, 1962) is hexagonal and the diffuse band is centred at 4.5 Å. A single difference can be noticed between the hexagonal structures of magnesium stearate and calcium stearate (C in Spegt and Skoulios, 1964): in the former, the long *d*-spacing value increases slightly with increasing temperature, whereas it decreases in the latter. The B phase of magnesium stearate is stable up to 190 °C.

More recently, Lelann and Bérar (1993) indexed the high resolution diffraction spectrum of calcium stearate *mono-hydrate* obtained by using a synchrotron X-ray source. Their results strongly suggest that the less resolved spectra obtained using conventional X-ray sources may lead to erroneous conclusions when they are used to infer crystal structures by lattice parameter refinement techniques.

Finally, as regard the structure of the room temperature forms of magnesium stearate, what is presently agreed upon is rather scarce: one parameter (noted *c* in the following) of the unit cell is much larger than the two others and the length of the long d_{001} spacing varies with water content in a way suggesting that the water molecules intercalate between the layers. The angle of inclination of the stearic chains over the interlayer planes containing the Mg ions and the carboxylic polar heads could, in principle, be inferred from the comparison of the length of the molecule and of the long spacing. For instance, in *anhydrous* Ca and Sr soaps, the long spacing increases proportionally with the length of the aliphatic chains (with carbon atom number ranging from 12 to 20 chains) and the later are perpendicular to the [0 0 1] planes (Spegt and Skoulios, 1964). However, the situation with magnesium soaps is not that clear, as can be seen by comparing the data collected in Table 1. The difference between the length of the long spacing d_{001} reported by Sharpe et al. (1997) for the trihydrates, dihydrates and anhydrates of pure magnesium stearate and pure magnesium palmitate, respectively, is not a constant. The inclination angle value that can be computed from it (the difference in length of stearic and palmitic chains being taken to be 2.54 Å) is also, in the case of the hydrates at least, physically inconsistent.

Table 1
Difference between long spacings values Δd_{001} and corresponding inclination angle computed from the data in Sharpe et al. (1997) for the different phases of magnesium stearate and magnesium palmitate

Phase	Δd_{001} (Å)	Inclination angle (°)
Anhydrates	4.1	54
Dihydrates	0.5	6
Trihydrates	2.0	23

2. Materials and techniques

Of the various commercial products previously investigated by the authors (Andrès et al., 2001) only those derived from vegetable raw products are considered here. They are hereinafter referred to as VF and VG where letters F and G come from their respective producer's names FACI and GREVEN, and V is a reminder of their vegetable origin. Analysis of the carboxylic chains has been performed by HPLC after conversion of the salt into free acids following the method recommended by the European pharmacopoeia and the results are expressed in weight of carboxylic acids. The combined palmitic and stearic acids content of both VF and VG amounts to 96.2±0.1 wt.% of all carboxylic acids formed, but the relative proportions differ, with 84 wt.% stearic acid in VF and 81.0 wt.% in VG. These figures correspond roughly to one palmitic chain for every six and five stearic chains in VF and VG, respectively.

Both VF and VG are analysed by X-ray diffractometry in their "as received" state and also after modification in the following conditions:

(a) degassing under high vacuum at either room temperature (RT in the following), here 25 (±2) °C, or 50 °C during several days as required for the pressure in the degassing chamber to return to its base value;
(b) ageing in an incubator at 25 (±0.1) °C in an atmosphere with 85 (±1)% RH, during periods of time ranging from 1 to 4 months. According to Sharpe et al. (1997), these later conditions should ensure the crystallisation of magnesium stearate trihydrate starting from the so-called anhydrate phase. However, it was observed that the crystallinity and water content of the samples aged under these conditions were not homogeneous, i.e. the production of single phase hydrates proved impossible in that way. Subsidiarily, this also made it impossible to infer from the following analyses any meaningful data about the kinetics of the hydration process.

All as received and modified materials are known to differ by their water content (Andrès et al., 2001). In different batches of the as received materials, the mean overall water content expressed in mole of water per mole of magnesium stearate and measured by the Karl Fisher technique (KF in the following) is found to be 1.80 (±0.13) in VF and 2.33 (±0.14) in VG. In a modified VF batch aged 2 months in the standardised conditions just mentioned, the stoichiometric ratio equals 2.29, corresponding to an uptake of 0.59 H_2O per magnesium stearate molecule. An important remark here is that the water content measured by the KF method systematically exceeds by about 0.5 H_2O per mole the result obtained by the infrared balance method following the standardised analysis conditions prescribed by the European pharmacopoeia (heating at 100 °C until constant weight). In the present case, heating up to 150 °C proved necessary to get agreement with the KF method.

The X-ray diffractograms were obtained by means of a 4096-channel position sensitive detector (CPS-120 from INEL) and Ni-filtered Cu Kα radiation. The acquisition window was 0.3–116° (2θ) and the resolution 0.029° (2θ) per channel. A numerical peak fitting procedure allowed doublet separation and evaluation of integral intensities with excellent accuracy.

X-ray diffractometry experiments at temperatures above RT have also been performed under dry nitrogen or helium atmosphere. For that purpose, the X-ray source and the position sensitive detector were mounted around a furnace equipped with beryllium foil windows and a sample holder designed to minimise the effect of its thermal expansion. Monochromated beams from either a cobalt or a copper anticathode were used.

3. Results

3.1. Room temperature X-ray powder diffractometry

The diffractograms of as received VF and VG in Fig. 1 reveal clear differences in the crystallisation and hydration states of both materials, as substantiated by the following considerations.

(a) The diffractogram of as received VF is in all respects similar to those reported in the literature for several as received commercial materials generally referred to as "anhydrates": spectra a and b in Fig. 1 of Leinonen et al. (1992), spectrum D in Fig. 3 of Müller et al. (1982) and spectrum labelled "Italy" in Brittain (1989). According to the different authors, it is typical of a *poorly crystallised* solid, the meaning of what is rather vague but will be clarified by the present work. The two low angle reflections (at 5.45 and 9.05–9.10° 2θ) can undoubtedly be identified with the [0 0 3] and [0 0 5] harmonics. One intense and large (2° 2θ FWHM) peak centred about 21.4° 2θ (referred to as line II in the following) is not assigned in the literature cited above. It looks very much like the diffraction band characteristic of the so called α or rotator form of many long chain fatty acids or their soaps, such as for instance the hexagonal phase of Ca-soaps as explained in Section 1.
(b) In contrast, the diffraction spectra of modified VF, e.g. aged one month, and that of as received VG exhibit fine diffraction lines. Among these, the harmonics of the [0 0 1] reflection, particularly those of 3rd and 5th order, are split into two components. The values of the d_{001} spacing that can be computed from the angular positions of

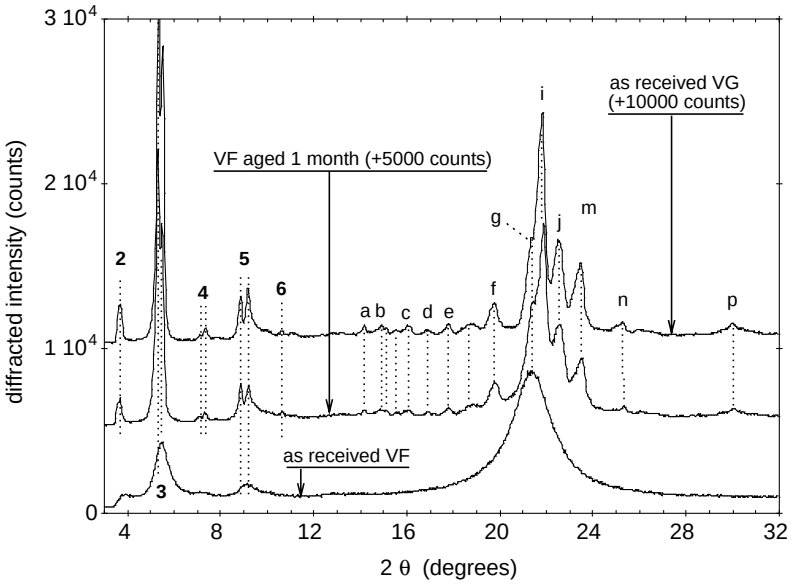

Fig. 1. X-ray diffractograms of as received VF, as received VG and modified VF (aged 1 month). X-ray beam wavelength: 1.5406 Å.

the *components* are in excellent agreement with those reported by Sharpe et al. (1997) (Table 2) for what these authors claim to be pure dihydrate and trihydrate phases, respectively. Accordingly, our materials would consist in mixtures of both phases. At higher diffraction angles, our diffractograms in Fig. 1 are comparatively much more structured. Very unfortunately, the corresponding section of the diffractogram of the pure dihydrates published by Sharpe et al. (1997) shows evidence of thermal alteration (probably during drying reportedly carried out at 55 °C) and cannot as a consequence be linearly combined to reproduce ours. In contrast, based on a visual evaluation, the two spectra labelled "United States" and "Germany" in Brittain (1989) look very much like the two required to reconstruct our own spectra by linear combination.

Table 2
d_{001}-Spacing value (in Å) as computed from the angular position of the successive harmonics of [0 0 1] diffraction peak (not observed)

Phase	Present work	Sharpe et al. (1997)	Vold and Hattiangdi (1949)	Ertel and Cartensen (1988)
Anhydrate	A: 47.36 (±0.06) [3, 4, 5, 6, 7] B: 48.34 (±0.13) [3, 5] C: 48.72 (±0.7) [3, 5]	48.81 (±0.25) [2, 3, 5]	47.00 (±0.24) (dried)	50.32 (±0.05)
Dihydrate	D: 48.11 (±0.07) [3, 4, 5] E: 48.25 (±0.13) [3, 4, 5]	48.11 (±0.20) [2, 3, 5]	49.3 (±0.15) (not dried)	52.20 (±0.03)
Trihydrate	D: 49.80 (±0.08) [3, 5] E: 49.84 (±0.09) [3, 5]	49.92 (±0.25) [2, 3, 5]		53.04 (±0.05)

When available, values of standard deviation and harmonics order are indicated between round and square brackets, respectively. (A): VG degassed at 50 °C under vacuum, diffraction pattern in Fig. 2. (B): VG degassed at 25 °C under vacuum, diffraction pattern in Fig. 2. (C): VF, as received, diffraction pattern in Fig. 1. (D): VG, as received; mixture of di- and trihydrate, diffraction pattern in Fig. 1. (E): VF, modified; mixture of di- and trihydrate, diffraction pattern in Fig. 1.

(c) In addition, the spectra of modified VF and as received VG in Fig. 1 being practically identical constitute evidence that the hydrated phases can be formed at room temperature by reaction of the "anhydrate" with water vapour.

(d) Conversely, the spectra of VG degassed at room temperature (Fig. 2) and of as received VF (Fig. 1) show the same features characteristic of the poorly crystallised "anhydrate" except for a different background intensity especially over the interval 10–18° 2θ. This is evidence that the hydrated phases can be dehydrated to a certain extent at room temperature under vacuum and their structure modified accordingly.

(e) A partly different diffractogram, shown in Fig. 2, and also in Fig. 3 is obtained by degassing the hydrated material VG under vacuum at 50 °C. In some sense, it is intermediate between the two types appearing in Fig. 1. At low diffraction angles (large d_{hkl}), the strong and fine [0 0 l] harmonics (numbered consecutively in the figure) are typical of a *single* very well crystallised layered phase, whereas, in the low d_{hkl} range 5–1 Å, it exhibits the same broad reflection as the poorly crystallised as received VF or as VG degassed at 25 °C. It looks also the same as the spectrum of the commercial USP grade from Hüls America Inc. published by Barra and Somma and labelled MgSt#12–14 in Fig. 4 of their article (Barra and Somma, 1996).

(f) At large diffraction angles not covered by Figs. 1 and 2, all spectra exhibit an additional weak band centred about 40° 2θ ($d_{hkl} \approx 2, 3$ Å). This is exemplified in Fig. 3 with the case of batch VG, to show the relationship between the fine bands in the well crystallised phase and the broad bands in the degassed sample. The latter seem to result from a degeneracy of the former about the same mean position and to be associated with the removal of water from the structure. In all diffractograms of concern in Figs. 1–3, the relative intensity of line III is 6–8% of that of line II (after background subtraction). It can also be noted that the total relative intensity of the set of [0 0 1] harmonics on the one hand with respect to that of lines II and III on the other appears as a highly variable characteristic of the diffractograms. But, in contrast, the relative intensity of the odd harmonics is *always much larger* than that of the even harmonics of next higher order.

(g) A recurrent question when dealing with commercial products, is associated with their actual purity. The composition of materials for pharmaceutical applications is standardised but, in the present case, the requirements regarding the presence and proportion of palmitic chains are low as reminded in the introduction. Accordingly, a fraction of palmitic chain (roughly 20% in weight) and a smaller fraction (roughly 20% in weight) of shorter chains is measured by HPLC. In relation with this, two remarks can be done. Firstly, no evidence of the presence of free crystallised stearic or palmitic acids could be found in any one of the diffraction spectra and all the characteristics just described above (in a–f) are incompatible with the assumption that the materials might consist of mixtures of *separate* stearate and palmitate phases. Secondly, in the spectrum of VG degassed at 50 °C, three fine lines of very small intensity (marked with an asterisk in Fig. 3) may constitute evidence of the presence of a second crystalline phase possibly associated with impurities since they are not noticed in other reports of lower resolution. They may be present also in the spectrum of the well crystallised as received material but until the structure of the hydrate phases is established this cannot be ascertained.

In conclusion of this descriptive section, an important final reminder may be that the water content of the well and poorly crystallised phases differs by only 0.6 mole H_2O per mole magnesium stearate, a surprisingly small figure when considering the structural consequences involved.

In Appendix A, the lattice-spacing and relative intensity values measured in the present work and reported in various references (ASTM, 1965; Brittain, 1989; Rajala and Laine, 1995; Sharpe et al., 1997) are listed. The data from reference (Brittain, 1989) are computed from the diffraction angles read from the reproductions of the diffraction spectra. Their original accuracy is thus reduced by an unknown amount. Based on the visual comparison of the different spectra or sequences of *d*-spacing values, it is

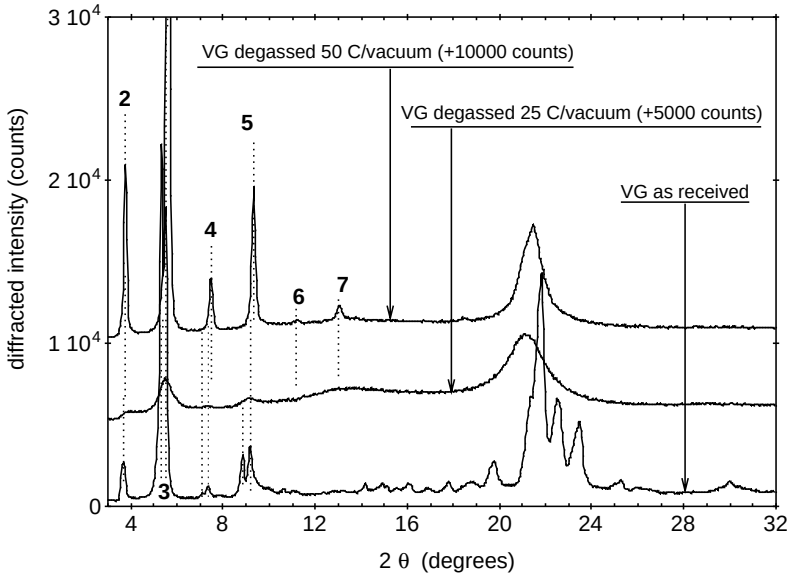

Fig. 2. X-ray diffractograms of as received VG, VG degassed at 25 and 50 °C. X-ray beam wavelength: 1.5406 Å.

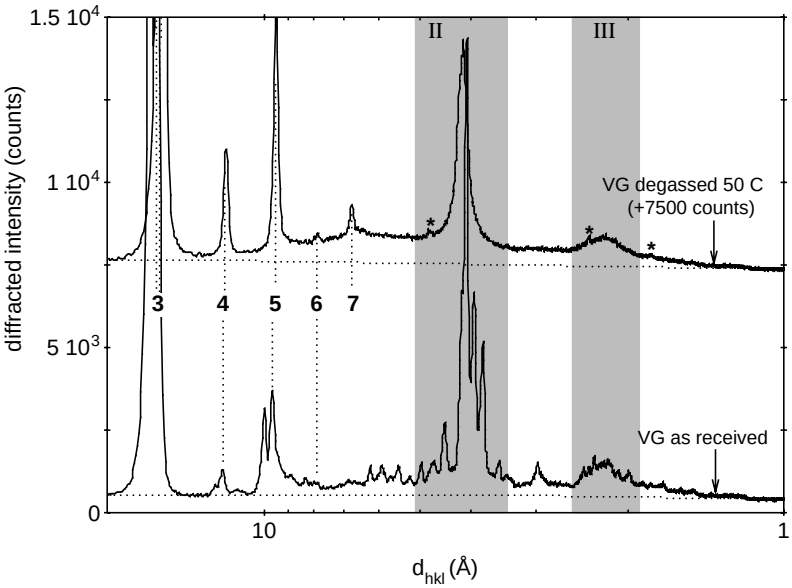

Fig. 3. Comparison of the X-ray diffractograms of VG as received and degassed at 50 °C showing the coincidence of the fine and broad diffraction bands II and III in both cases.

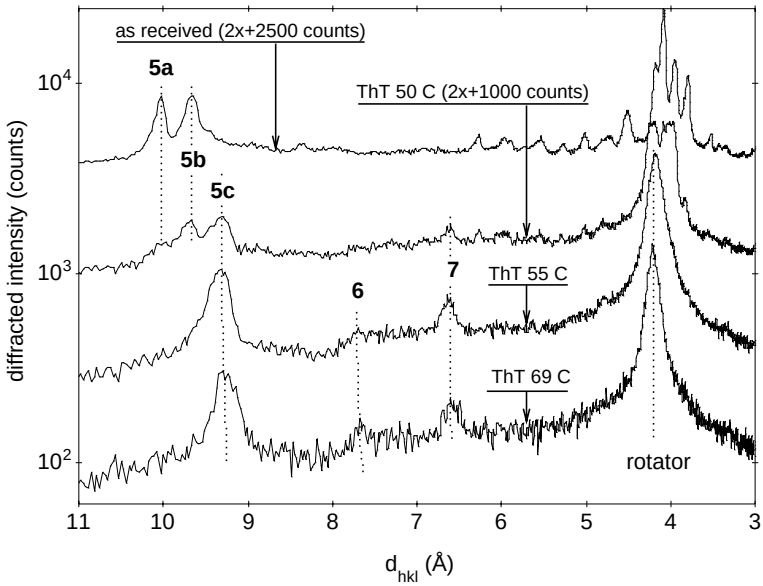

Fig. 4. X-ray diffractograms of as received VG after one hour isothermal treatment at increasing temperature under dry nitrogen. The upper two curves are multiplied and shifted as indicated. The labels 5a, 5b and 5c refer to the (0 0 5) harmonic of the trihydrate, dihydrate and anhydrate phase, respectively, in accordance with the data in Table 2.

very likely that there are only two distinct diffraction spectra representative of the well crystallised hydrated phases and that they can be assigned to the dihydrate and trihydrate. Textural effects (particle preferential orientation) is a source of additional complication.

3.2. High temperature X-ray diffactometry

Fig. 4 shows a set of diffractograms obtained by analysing a VG sample sequentially at increasing temperature. At each temperature step, spectrum acquisition has been started after one hour thermal equilibration. Notice the logarithmic ordinate scale in the figure and the fact that the two upper spectra are dilated by a factor 2. It is evident that the transformation of the initial structure of as received VG takes place gradually. Close inspection of the [0 0 5] harmonic profile shows a succession of three structural phases. Based on the data in Table 2, it can be inferred that the trihydrate disappears first, next the dihydrate to yield at 55–69 °C, the best crystallised form of the "anhydrate" similar to the one obtained after long time treatment at 50 °C under vacuum and return to RT. The modifications in the spectrum recorded after thermal treatment at 55 °C as compared to 50 °C are indication that the dehydration process is not complete after one hour treatment at 50 °C and is a thermally activated process. Notice that these modifications include a substantial improvement of the signal to noise ratio which is not obvious in the figure due to the different intensity scale of the two spectra.

At higher temperatures, the anhydrate structure is subject to further modifications. Up to about 100 °C, the essential observation is that the diffraction band II shifts towards larger d_{hkl} values. This is demonstrated in Fig. 5 which compares averaged spectra obtained at 55 and 100 °C using NaCl as an internal standard. The positions of the diffraction lines of NaCl remain unchanged while the a rotator band shifts by some 0.2 Å. It can also be observed in Fig. 5 that the *profile* of the diffraction band is modified. The line is the narrowest at the highest temperature. Notice again the very low intensity diffraction line marked with asterisks at the same positions as in Fig. 3.

All values of the central position of the diffraction band of the rotator phase determined in three distinct experiments are plotted in Fig. 6. Experiment #3

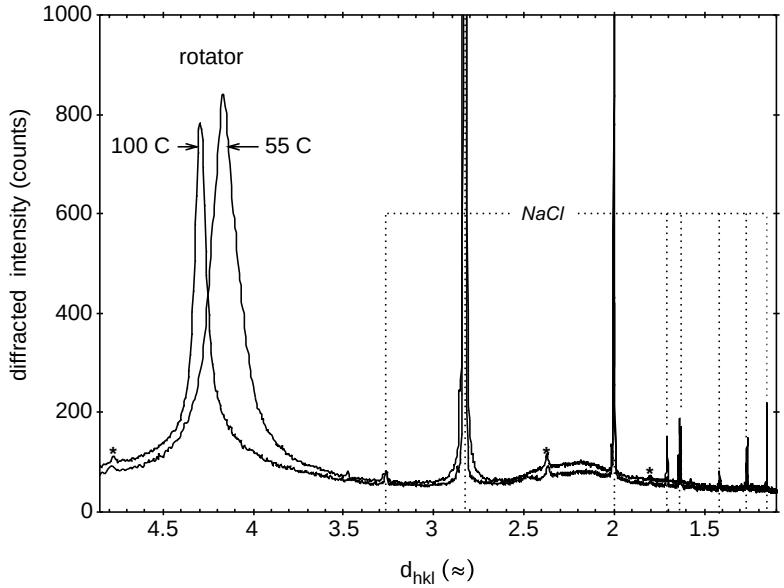

Fig. 5. Averaged X-ray diffractograms of as received VG recorded at 55 and 100 °C. As temperature is increased the diffraction band of the rotator phase shifts to a larger *d* value and its width decreases. The position of the diffraction lines of the internal standard NaCl is stable.

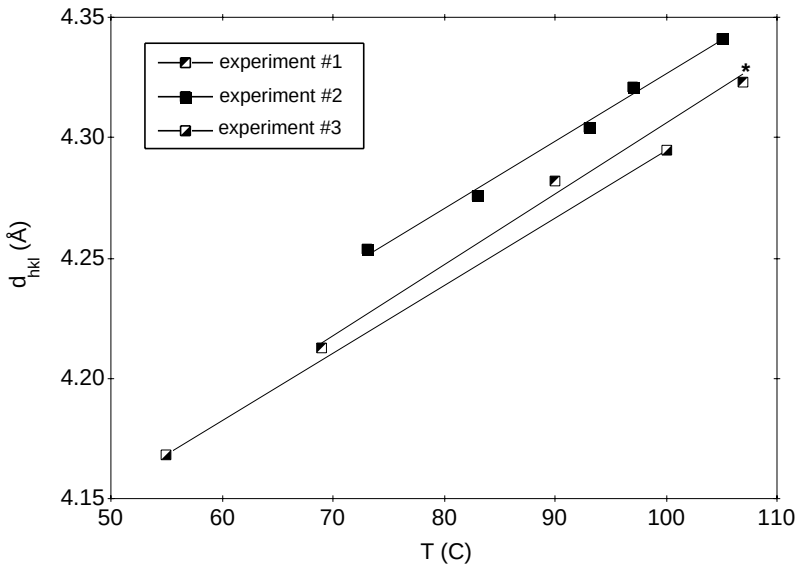

Fig. 6. Temperature dependence of the *d*-spacing measured at position of maximum of rotator diffraction band II. Experiment #3 refers to the diffractograms shown in Fig. 5. The data points of experiments #1 and #2 have been obtained from a single diffractogram each. The point at 107 °C marked with an asterisk shifts to 4.356 Å after 15 h (see Fig. 8).

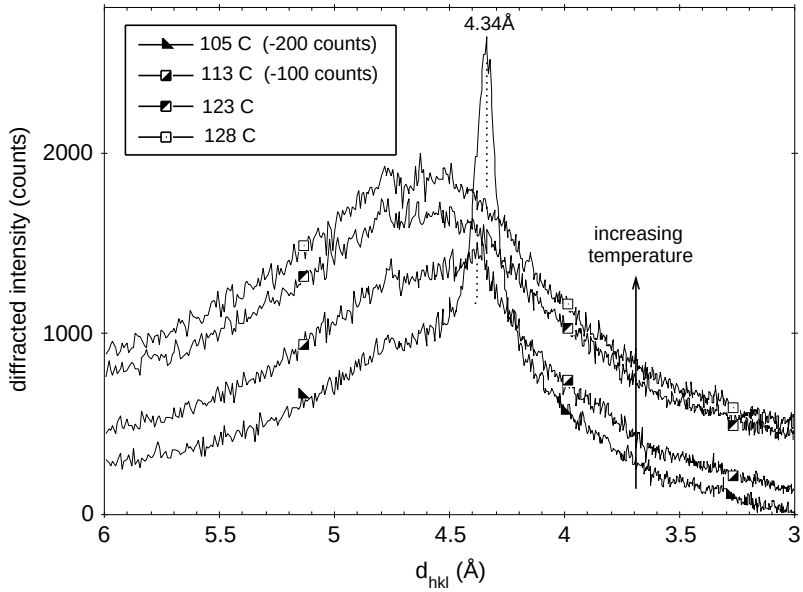

Fig. 7. Gradual transition from the diffraction band II of the rotator phase to the diffusion band of the melted chains, as temperature is increased.

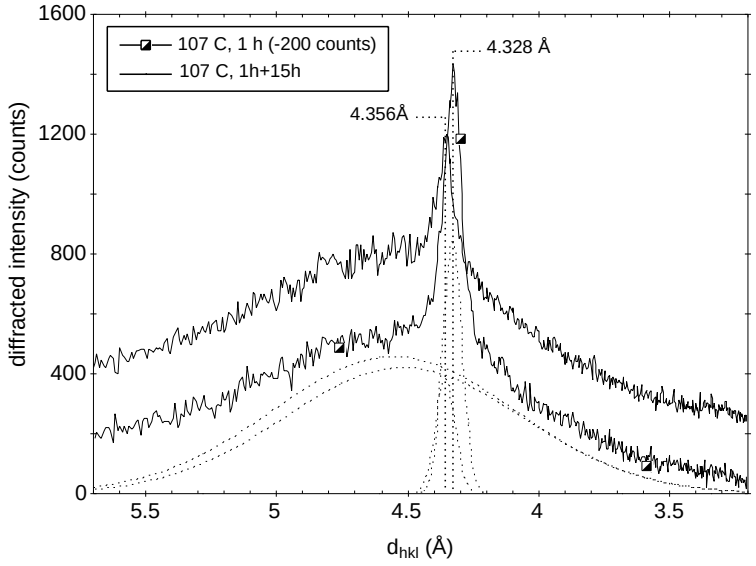

Fig. 8. Gradual transition from the diffraction band II of the rotator phase to the diffusion band of the melted chains, with increasing isothermal treatment duration.

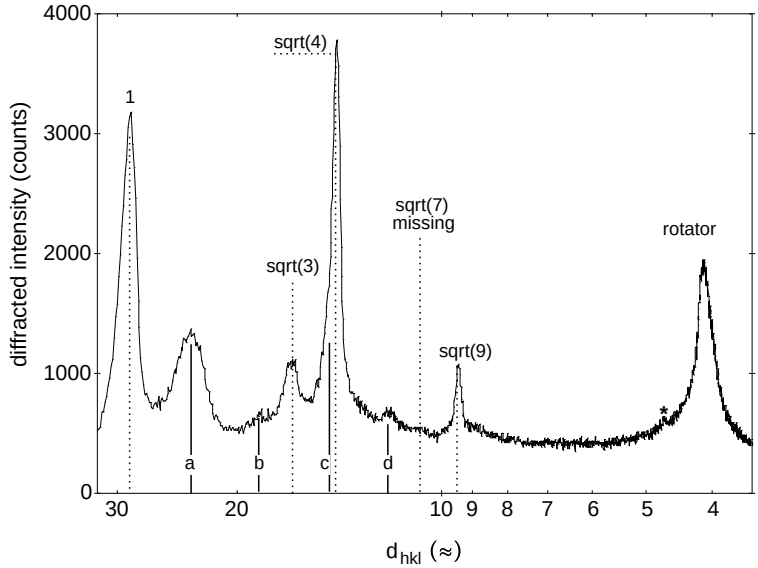

Fig. 9. Diffractogram recorded at room temperature after melting of batch VG at 130 °C followed by slow cooling.

corresponds to the data in Fig. 5. Experiments #1 and #2 has been carried out without addition of an internal standard. The trend is in all three cases qualitatively similar and corresponds to an average value of the dilation coefficient equal to 6.9×10^{-4} ($\pm 1.6 \times 10^{-4}$). As obvious from the following, the data point at the highest temperature (107 °C) shifts upwards (towards higher values) with increasing duration of the isothermal treatment.

Above roughly 100 °C, Fig. 7 shows how line II gradually disappears to the benefit of a much broader diffusion band with gaussian profile, centred around $d_{hkl} = 4.62$ Å. According to general knowledge about lipids, the latter is characteristic of liquid "fatty chains" (chain melting).

As shown in Fig. 8, the *isothermal* "melting" of the rotator phase can also be monitored by the gradual collapse of its diffraction band and the reverse built-up of the diffuse band due to the liquid state as in Fig. 7. Obviously, this is still a very slow process at 107 °C since the rotator phase is still observed after 15 h. Notice that the same observation could be repeated at other temperatures (results not shown). The diffracted intensity profiles in Fig. 8 are satisfactorily modelled by the sum of two gaussian components shown as dotted curves (background subtracted). The respective width at half-maximum of these components differ by roughly a factor of 10.

As can be seen in Fig. 7, when the temperature has reached about 130 °C, only the diffusion band remains visible and the material can be considered as melted. After cooling down to room temperature, the diffraction spectrum is as shown in Fig. 9. The rotator band now replaces the diffusion band and a different set of fine diffraction lines can be observed at low diffraction angles. The lines labelled 1, sqrt(3), sqrt(4), sqrt(9) might correspond to the (quenched) hexagonal phase mentioned in the Section 1.

4. Discussion

Commercial magnesium stearate is available as either crystalline hydrates (here a mixture of the di- and trihydrates, and rarely as a single phase) or a so called poorly crystallised "anhydrate" depending on whether it has been dried or not, and if so in which conditions. This is in accordance with many previous reports (Vold and Hattiangdi, 1949; Brittain, 1989; Sharpe et al., 1997), but the so called anhydrate phase contains a significant amount of water corresponding roughly to one mole H_2O per mole of magnesium stearate. It

has been demonstrated elsewhere that such an amount *cannot* be accounted for by physical adsorption on the particles outer surface (Andrès et al., 2001). Actually, the crystallisation of the di- and trihydrate mixture from the "anhydrate" exposed to humid air, as appears in Fig. 1, requires an uptake of only about 0.6 mole H_2O per mole stearate. This can take place at room temperature under sufficient water partial pressure, in agreement with literature (Sharpe et al., 1997). The reverse transformation of the hydrates into the "anhydrate" can be carried out under vacuum at room temperature or at increasing temperature under vacuum or dry gas. Vold and Hattiangdi (1949) already obtained the same result by drying at room temperature in presence of P_2O_5 and in ambient air at 90 °C. In fact, it is essentially this low temperature reactivity toward water vapour that requires clarification in structural terms.

Schematically, the diffractograms of the crystallised hydrates consist in three bands of fine reflections (including the [0 0 *l*] harmonics) and of a set of weak and very weak reflections between the first and second bands. They could not be successfully indexed by using Vand's graphical methods. The very likely reason of that failure is that the crystallised materials are two-phase mixtures, of the di- and trihydrate as substantiated in Section 3.1. Using the data listed in table of appendix, an attempt was made to separate the observed set of d_{hkl} values in two subsets, each corresponding to a different hydrate structure. Indexing each subset by Vand's method again proved unsuccessful. The potential solutions should likely belong either to the triclinic crystal system, as proposed for magnesium palmitate (Sharpe et al., 1997) based on indirect evidence, or to the orthorhombic or monoclinic systems, according to Müller (1977a). Using the unit cell parameter values and crystal system *proposed by the later* as recalled in Section 1, and considering the extinction rules of all allowed space groups in the orthorhombic and monoclinic systems successively, failed to generate a set of *d*-spacing values showing coincidence with all experimental values in any one of above two subsets.

Based on the density values evaluated by helium pycnometry and reported in Fig. 1 of Andrès et al. (2001), it is possible to evaluate the densities of the di- and trihydrate to 1.06 and 1.10 g cm^{-3}, respectively. Accordingly, and if the two structures were belonging to the same orthorhombic or monoclinic crystal system, the volume of a unit cell containing one molecule would differ very little and the product of the two small lattice parameters (*a* and *b*) by 4% only. Thus, the probability that homologous diffraction lines (allowed by the extinction conditions of each structure) overlap and be experimentally unresolved would be very high.

The different intensities of the [0 0 *l*] harmonics of even and odd order can be qualitatively interpreted, independently of solving the structure, on a simple basis developed by Schearer (1925). This cannot provide additional structural information and is just in qualitative agreement with the accepted end-to-end arrangement of the molecules in successive layers.

The projected length of the stearic chain starting from the carbon atom of the carboxyl head including the length of the terminal methyl group can be estimated at 23.9 Å. If two stearic chains are aligned end to end, perpendicular to the {0 0 1} plane, their added lengths make almost exactly for the d_{001} spacing of the anhydrate phase A or B in Table 2. In that case, the O–Mg–O bonds would have to lie parallel to the {0 0 1} plane. Otherwise, the direction of the chains should make an acute angle with the normal to the same plane. Clearly, structural information is lacking to decide which situation actually prevails and this precludes our precise understanding of the positioning of the water molecules within the structures, a key point if the question of whether the lubricity of the material is structure-dependent or not, is to be answered. As a first step, obviously, additional X-ray diffraction experimental investigation and possibly computational modelling are mandatory if the mechanism of the reaction of water with magnesium stearate is to be elucidated.

When the hydrates are dehydrated in the XRD-furnace at increasing temperature, the fine diffraction bands II and III are observed to degenerate gradually into the two broad lines II and III, characteristic of the rotator or α form, in which the plane containing the carbons of each stearic chain are assumed to rotate freely around the direction of the chain. This gradual modification of the profile of diffraction band II as it appears in Fig. 4 at 50 °C, provides one with an obvious explanation to the variability of that section

of the diffraction spectra reported in the literature, as the result of the partial thermal degradation by heat drying.

What is puzzling here is that the thermal degeneracy of the diffraction band can be achieved by the removal of water at room temperature. In this respect, temperature appears now as a parameter of secondary or no importance, as long as the formation of the rotator phase is concerned in the particular case of magnesium stearate. It looks as if the water molecule, when inserted between the polar heads of two or more stearate molecules, was capable to quench the rotation of the chains and conversely loosen it when leaving the structure. From the standpoint of logic, this appears to be a nonsense unless one accepts the idea that it is the entire stearate molecules including their polar head that are made free to rotate or not. That purely speculative consideration is presented here to emphasise how interesting it would to fully understand the mechanism of the reaction of such layer structure with water.

In the diffractograms of the anhydrates recorded at room temperature (Figs. 1 and 2), the ratio of the intensity of line III relative to that of line II remains roughly constant and independent of the changes observed in the profile and intensities of the [0 0 *l*] harmonics. In contrast, the ratio of the (total) X-ray intensity of the [0 0 l] harmonics over that of the broad lines II and III *is* changing (increasing with the degassing temperature), while, as confirmed by results of thermal-gravimetric analysis to be published separately, the water content remains unchanged. The finer profile of the [0 0 *l*] harmonics is indicative of larger coherent diffraction domains and/or lower lattice micro-strains in the direction of *c*-axis. This is indication that the elimination of (only) a fraction of the water from the crystalline hydrates at room temperature (1.2 molecule from between two Mg-stearate molecules) leaves a relatively disordered structure also along that direction.

The melting of the stearic chains is revealed by the gradual disappearance of the rotator line II and the growth of a broadest band with gaussian profile: the width of the rotator diffraction band is multiplied by a factor of 10. The process starts above 100 °C and it will be shown in a subsequent publication dealing with the thermal analyses of the same materials, that the details of the associated thermal events up to full melting are strikingly different depending on whether the starting material has been degassed before hand at 25 or 50 °C or is generated in situ from the hydrated batches. The X-ray investigation of the product obtained by cooling and solidification of the melted sample (Fig. 9) has no counterpart in the literature. Apart from the three weak diffraction lines (already appearing on heating in Fig. 3 and that remain present) the diffractogram seems to reveal two crystallised phases. Additional experiments and specific literature review would be needed to develop an interpretation but the presented data has the merit of further emphasising the physical–chemical complexity of the system of concern and possibly raising interest for its investigation.

5. Conclusion

A detailed description of the X-ray powder diffractograms and their reversible modifications with temperature or relative humidity of both crystallised (hydrate) and poorly crystallised (anhydrate) forms of magnesium stearate has been given. The broad qualitative agreement with literature on the change from the hydrate to the anhydrate type is evidence that the underlying structural property is independent of the origin of the material. Structural differences between commercial materials seem to be almost uniquely determined by their degree of hydration in relation with the production, drying and storage conditions.

The additional information derived from the X-ray diffraction experiments performed at temperatures above RT and by investigation of the literature relative to other metal soaps allows a novel and interesting conclusion. The broad diffraction band around $d_{hkl} = 4.15$ Å, at RT can formally be regarded as the precursor of the a rotator band which can only be observed in other metal soap systems at higher or much higher temperature. Its reversible transition to the fine diffraction band of the hydrates associated with the reversible incorporation of water in the structure (by intercalation between the layers) is indicative of a yet unnoticed link between the number of water molecules present and the capacity for the plane of the aliphatic chain to rotate freely or not around their longitudinal direction.

Appendix A. *d*-Spacing values observed in present work using high resolution position sensitive counter

n or label	Present work			ASTM (1965)		Sharpe et al. (1997)				Rajala and Laine (1995)		Brittain (1989)	
	d_{hkl} (Å)	2θ	I/I_0	d_{hkl} (Å)	I/I_0	d_{hkl} (Å) dihydrate	I/I_0 dihydrate	d_{hkl} (Å) trihydrate	I/I_0 trihydrate	d_{hkl} (Å) dihydrate	I/I_0 dihydrate	d_{hkl} (Å) "USA"	d_{hkl} (Å) "Germany"
2	24.588	3.5905	3.4	26.500	20			25.066	45.4				
2	23.854	3.7010	4.6			24.143	50.5						
3	16.656	5.3014	61	17.650	50			16.667	100				17.02
3	16.076	5.4930	35.7			16.048	100					16.70	
4	12.476	7.0799	0.8					12.295	1.7	12.93	15		
4	12.054	7.3279	2.4			12.061	6.2						
5	9.9835	8.8504	8.6	10.52	5			9.9279	6.4	10.37	100		10.24
5	9.6228	9.1828	8.3			9.5797	13.5					9.89	
	≈8.84?	≈10		8.85	2					8.67	6		
	8.3314	10.610	11.7					8.4253	2.7			8.25	
	≈8.04	≈11											
				7.5910	2					7.43	7		
				7.0660	1							7.09	
				6.5920	10			6.3802	2.2	6.51	31	6.41	
	6.2511	14.157	1.9										
a	5.9962	14.762	2.5										5.96
b	5.9424	14.896	1.1	6.0360	5								5.96
	5.8606	15.105	0.7	5.8060	2								
	5.6986	15.537	1.2	5.6860				5.7122	1.4				
c	5.5267	16.024	3.1	5.5300						5.54	2		
										5.34	15		
										5.29	27		
d	5.2516	16.869	0.9	5.2550	3					5.21	32		
								5.1069	2.3				5.11
e	4.9893	17.763	2.7	5.0030						5.04	1		
										4.84	3		
										4.79	6		
	4.7308	18.742	4.3	4.7260						4.74	5	4.70	
f	4.4934	19.742	15	4.4830	100			4.5369	19.4	4.44	12		4.51
				4.3760	1					4.35	22		
g	4.1436	21.427	66.7	4.1870	1	4.1989	60.1	4.2077	25.3	4.09	23	4.20	4.21
i	4.0774	21.779	40.9	4.0570	20					4.07	23	4.09	4.08
	4.0528	21.913	60.9							4.03	19		

j	3.9356	22.574	59.3	3.9450	1					3.95	2	3.96		
j′	3.8203	23.265	22.9					3.8240	16.5	3.78	20		3.82	
m	3.7761	23.541	28.7	3.7840	100	3.8047	7.1			3.73	16			
				3.6970	1									
n	3.5271	25.229	6.3	3.5190	5	3.5676	1.6			3.54	6		3.54	
				3.4242						3.48	9	3.41		
				3.3470	1					3.31	8			
										3.27	14			
				3.1530	1					3.17	1			
				3.0360	1					3.07	6			
p	2.9704	30.060	12	2.9840	2								2.99	
				2.7790	1									
				2.7140	1									
q	2.4245	37.050	2.5	2.4240	5								2.45	
r	2.3718	37.903	1.5	2.3580	1									
s	2.3127	38.910	3.7	2.2850	2								2.24	
	2.2214	40.578	100										2.21	
t	2.1673	41.637	2.5	2.1930	5							2.17	2.17	
				2.1250	1									
u	2.0773	43.533	0.8	2.0870	2							2.09	2.09	
				1.9970	2									
v	1.9845	45.679	9.5	1.9740	2								2.00	
w	1.8799	48.378	1.6	1.8870	2								1.89	
				1.8520	1									
				1.7680	1									
	1.6991	53.919	0.7											
	1.5773	58.467	0.6											

Comparison with values reported in the literature. Letters from first column to identify the short *d*-spacing values are in accordance with labels in Fig. 1. Data in last two columns (Brittain, 1989) are computed from the angular positions read from figures.

References

American Society for Testing and Materials, 1965. Powder diffraction file, file 5-0292.

Andrès, C., Bracconi, P., Pourcelot, Y., 2001. On the difficulty of assessing the specific surface area of magnesium stearate. Int. J. Pharm. 218, 153–163.

Barra, J., Somma, R., 1996. Influence of the physicochemical variability of magnesium stearate on its lubricant properties: possible solutions. Drug Dev. Ind. Pharm. 22, 1105–1120.

Brittain, H.G., 1989. Raw materials. Drug Dev. Ind. Pharm. 15, 2083–2103.

Ertel, K.D., Cartensen, J.T., 1988. Chemical, physical and lubricant properties of magnesium stearate. J. Pharm. Sci. 77, 625–629.

European Pharmacopeia, 2002. Magnesium stearate. Direction Européenne de la Qualité des Médicaments, 4th ed. pp. 1647–1649.

Leinonen, U.I., Jalonen, H.U., Vihervaara, P.A., Laine, E.S.U.J., 1992. Physical and lubrication properties of magnesium stearate. Pharm. Sci. 81, 1194–1198.

Lelann, P., Bérar, J.-F., 1993. Synchrotron high resolution powder study of molecular packing in hydrate calcium stearate. Mat. Res. Bull. 28, 329–336.

Marwaha, S.B., Rubinstein, M.H., 1988. Structure-lubricity evaluation of magnesium stearate. Int. J. Pharm. 43, 249–255.

Müller, B.W., 1977a. The pseudo-polymorphism of magnesium stearate. In: First International Conference on Pharmacy Technology, Paris, May 31–June 2, pp. 134–141.

Müller, B.W., 1977b. Tribologische Gesetzmässigkeiten und Erkenntnisse in der Tablettentechnologie. 3: Untersuchungen an reinen Magnesium- und Calciumstearaten. Pharm. Ind. 39, 161–165.

Müller, B.W., 1977c. Die Pseudo-Polymorphie von Magnesiumsalzen höherer Fettsäuren. Arch. Pharm. 310, 693–704.

Müller, B.W., Steffens, K.-J., List, P.H., 1982. Tribologische Gesetzmässigkeiten und Erkenntnisse in der Tablettentechnologie. 6: Einflüsse physikalisher Eigenschaften chemisch reiner Magnesiumstearate auf die Schmiereigenshaften bei der Tablettierung. Pharm. Ind. 44, 729–734.

Rajala, R., Laine, E., 1995. The effect of moisture on the structure of magnesium stearate. Thermochim. Acta 248, 177–188.

Schearer, G., 1925. On the distribution of intensity in the X-ray spectra of certain long-chain organic compounds. Proc. Roy. Soc. Lond. A 108, 655–666.

Sharpe, S.A., Celik, M., Newmann, A.W., Brittain, H.G., 1997. Physical characterization of the polymorphic variations of magnesium stearate and magnesium palmitate hydrate species. Struct. Chem. 8, 73–84.

Small, D.M., 1986. Handbook of Lipid Research. The Physical Chemistry of Lipids. Plenum Press, New York.

Spegt, P.A., Skoulios, A.E., 1960. Structure des phases mésopmorphes du stéarate de calcium anhydre. CR Acad. Sci. Paris 251, 2199–2201.

Spegt, P.A., Skoulios, A.E., 1962. Structure des phases mésomorphes du stéarate de magnésium. CR Acad. Sci. Paris 254, 4316–4318.

Spegt, P.A., Skoulios, A.E., 1964. La structure des colloïdes d'association. X. description de la structure des savons de calcium à température ordinaire et à température élevée. Acta Cryst. 17, 198–207.

Vand, V., 1948a. Indexing method of powder photographs of long-spacing compounds. Acta Cryst. 1, 109–115.

Vand, V., 1948b. A third graphical method of indexing powder photographs of long-spacing compounds. Acta Cryst. 1, 290–291.

Vold, R.D., Hattiangdi, G.S., 1949. Characterisation of heavy metal soaps by X-ray diffraction. Ind. Eng. Chem. 41, 2311–2320.